AB

Nijmegen preprint
HEN-393
September 1996

# Reactions with leading hadrons in meson-proton interactions at 250 GeV/*c*

EHS/NA22 Collaboration

CERN LIBRARIES, GENEVA
SCAN-9612054

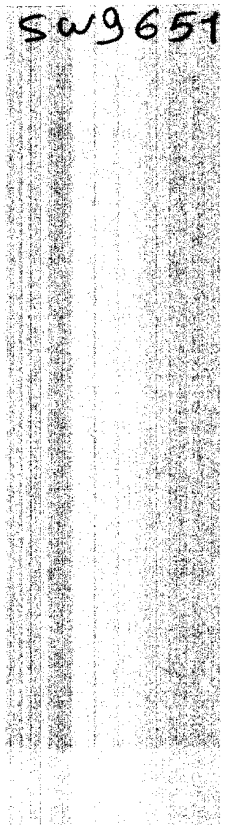

Nijmegen preprint
HEN-393
September 1996

# Reactions with leading hadrons in meson-proton interactions at 250 GeV/$c$

EHS/NA22 Collaboration

N.M. Agababyan[7], M.R. Atayan[7], E.A. De Wolf[1,a], K. Dziunikowska[2,b], A.M.F. Endler[5], Z.Sh. Garutchava[6], H.R. Gulkanyan[7], R.Sh. Hakobyan[7], J.K. Karamyan[7], D. Kisielewska[2,b], W. Kittel[4], S.S. Mehrabyan[7], Z.V. Metreveli[6], K. Olkiewicz[2,b], F.K. Rizatdinova[3], E.K. Shabalina[3], L.N. Smirnova[3], M.D. Tabidze[6], L.A. Tikhonova[3], A.V. Tkabladze[6], A.G. Tomaradze[6,c], F. Verbeure[1], S.A. Zotkin[3]

[1] Department of Physics, Universitaire Instelling Antwerpen, B-2610 Wilrijk, Belgium
[2] Institute of Physics and Nuclear Techniques of Academy of Mining and Metallurgy and Institute of Nuclear Physics, PL-30055 Krakow, Poland
[3] Nuclear Physics Institute, Moscow State University, RU-119899 Moscow, Russia
[4] High Energy Physics Institute (HEFIN), University of Nijmegen/NIKHEF, NL-6525 ED Nijmegen, The Netherlands
[5] Centro Brasileiro de Pesquisas Fisicas, BR-22290 Rio de Janeiro, Brazil
[6] Institute for High Energy Physics of Tbilisi State University, GE-380086 Tbilisi, Georgia
[7] Institute of Physics, AM-375036 Yerevan, Armenia

## Abstract.

Inelastic final states with one or two leading hadrons are studied in $\pi^+$p and $K^+$p interactions at 250 GeV/$c$. In reactions with two leading hadrons, the dependence of the average charge multiplicity of associated pions on their effective mass is essentially consistent with that observed in $\bar{p}$p and $\gamma\gamma$-collisions, but differs from that obtained in $e^+e^-$-annihilation. The multiplicity and (semi)inclusive characteristics of the $\pi^+$-induced non-diffractive reactions are compared to predictions of current versions of the FRITIOF fragmentation model. We show that the hard-like sub-processes, essentially responsible for the production of leading hadrons with relatively large transverse momentum as well as for the relatively large multiplicity of associated pions, are not properly treated in the model.

[a] Onderzoeksleider NFWO, Belgium
[b] Supported by the Polish State Committee for Scientific Research
[c] Now at UIA, Wilrijk, Belgium

# 1 Introduction

One of the characteristic features of multiparticle production, in $e^+e^-$-annihilation or lepton-nucleon scattering as well as in hadron-hadron collisions, is the increase of the role of hard-like effects with increasing collision energy $\sqrt{s}$. In particular, these effects give rise to a scaling violation observed in the Feynman-$x$ dependence of the average transverse momentum $\langle p_T \rangle$, the lifting of the so-called "sea-gull" wings with increasing $\sqrt{s}$ [1–4].

In deep-inelastic processes initiated by non-composite particles (leptons), the non-scaling effects can be successfully described by hard gluon emission from one or two leading (current) quarks. The physical picture of the interaction of composite particles (hadrons) is more complicated. Nevertheless, it can be supposed that even in that case the non-scaling effects derive from hard-like phenomena, such as parton-parton scattering and gluon radiation [5, 6].

The consideration of these types of sub-processes in the recently proposed version of the FRITIOF fragmentation model [6] allows for the reproduction of the charged particle multiplicity and single-differential inclusive distributions in high-energy hadronic collisions. As has been shown for meson-proton interactions at 250 GeV/$c$ [7], the model fails, however, to reproduce the double-differential spectra (the $x$-dependence of $\langle p_T \rangle$) for both single particles and hadron systems, since it predicts a $\langle p_T \rangle$ that is too small in the fragmentation regions. The inconsistency between model and data is most evident for leading hadrons ($|x| > 0.5$), the largest fraction of which are known to be identical to the incident hadrons (e.g. a proton at $x < -0.5$ and a $\pi^+(K^+)$ meson at $x > 0.5$ for the case of $\pi^+(K^+)$p-interactions). A more detailed experimental study of hadronic final states with leading hadron(s) is, therefore, expected to provide new information on the underlying hard-like effects necessary for the improvement of the model predictions.

This work, therefore, is devoted to the study of the properties of leading-hadron production in $\pi^+$p and $K^+$p-interactions at 250 GeV/$c$. The experimental procedure is described in Sect. 2. In Sect. 3, we present the dependence of the average charged particle multiplicity $\langle n \rangle$ of the associated central hadron system $X_n$ on the effective mass $M_X$ of this system for the reactions

$$\pi^+ p \rightarrow \pi^+_{lead}\, p_{lead}\, X_n \quad (1)$$

$$K^+ p \rightarrow K^+_{lead}\, p_{lead}\, X_n \ , \quad (2)$$

compared to that measured in other hadron-hadron, $e^+e^-$ and $\gamma\gamma$-collisions. In Sect. 4, the pion induced single-leading-hadron processes

$$\pi^+ p \rightarrow p_{lead}\, X_n(\text{non-leading}) \quad (3)$$

$$\pi^+ p \rightarrow \pi^+_{lead}\, X_n(\text{non-leading}) \quad (4)$$

are studied and compared to the FRITIOF-model predictions. The results are summarized in Sect. 5.

# 2 Experimental procedure

The experiment (NA22) was performed at CERN in the European Hybrid spectrometer equipped with the Rapid Cycling Bubble Chamber (RCBC) and exposed to a 250 GeV/$c$ tagged positive meson-enriched beam. The experimental set-up and the trigger conditions are described in detail in [8–10]. Charged-particle momenta are measured over the full solid angle with an average resolution varying from 1-2% for tracks reconstructed in RCBC and 1-2.5% for tracks reconstructed in the first lever arm, to 1.5% for tracks reconstructed in the full spectrometer. Ionization information is used to identify protons up to 1.2 GeV/$c$ and electrons (positrons) up to 200 MeV/$c$. All unidentified tracks are given

the pion mass, except the fast ($x > 0.5$) positive particle in the kaon induced reaction (2), where it is given the kaon mass.

Events are accepted when the measured and reconstructed charge multiplicity are consistent, charge balance is satisfied, no electron (positron) is detected and the number of tracks of bad quality is restricted to 0,1,1,2 and 3 for charge multiplicity 2,4,6,8 and > 8, respectively. Additionally, it is required that tracks corresponding to leading hadrons ($|x| > 0.5$) belong to the properly reconstructed ones, and that the system $X_n$ in (3) and (4) does not contain a leading hadron (i.e., a $\pi^+$ with $x > 0.5$ in (3) or an identified proton with $x < -0.5$ in (4)). Candidates for elastic scattering, selected according to the criteria described in [11] and [12], are excluded from the analysis. We have also excluded events of the type (1), (2) and (4) with low squared four-momentum transfer to the leading meson ($|t_{M\to M}| < 0.05$ GeV$^2$), as the trigger efficiency is very low for these events.

After these cuts, the sample with two leading hadrons consists of 2947 events of type (1) and 1702 events type (2). In Sect. 3, the non-diffractive processes of reaction (1) in particular are considered. A candidate for diffraction dissociation contains at least one leading hadron with $|x| > 0.88$ and no more than 6 charged particles in the final state [13]. The non-diffractive sample contains 1252 events of type (1). The non-diffractive samples of types (3) and (4), considered in Sect. 4, contain 7468 and 9903 events, respectively.

The events are weighted to correct for losses induced by the interaction trigger [11]. They are also given a multiplicity-dependent weight which corrects for the fraction of badly reconstructed (and therefore excluded) events.

The effective mass of the system $X_n$ produced in (1) and (2) is calculated as

$$M_X^2 = (p_1 + p_2 - p_p - p_M)^2/c^2, \tag{5}$$

where $p_1$ and $p_2$ are the four-momenta of the incident particles, $p_p$ and $p_M$ those of the leading proton and leading meson, respectively. Similarly, for (3) and (4), we use

$$M_X^2 = (p_1 + p_2 - p_p)^2/c^2 \text{ and } M_X^2 = (p_1 + p_2 - p_M)^2/c^2 \ , \tag{6}$$

respectively.

# 3 Reactions with two leading hadrons

## 3.1 The effective mass dependence of the average multiplicity

In Fig. 1, our data on average charged particle multiplicity $\langle n \rangle$ of the hadronic system $X_n$, produced in reactions (1) and (2), are presented as a function of the effective mass $M_X$ of this system and compared to the available data obtained for hadron-hadron collisions at lower incident momentum (147 GeV/$c$ for $\pi^+$p and K$^+$p-collisions [14] and 32 GeV/$c$ for $\bar{\text{p}}$p-collisions [15]), and for e$^+$e$^-$ [16–19] and $\gamma\gamma$-collisions [20] in the relevant effective mass range of the final hadron system. In [14] and [15] the leading hadrons are required to have $|x_{\text{lead}}| > 0.3$, while the more stringent cut-off of $|x_{\text{lead}}| > 0.5$ is applied in our work.

As can be seen from Figs. 1a and 1b, the average multiplicity $\langle n \rangle$ depends on the effective mass, but not on the projectile momentum or on the Feynman-$x$ cut. The discrepancy between the data of [14] and the present data at $M_X < 2$ GeV/$c^2$ is due to different selection criteria for 2-prong events ($n$=0), the relative contribution of which is more significant in the small $M_X$ region than it is in the large $M_X$ one.

The sub-sample of events with both leading hadrons carrying the major part of the incident momentum, $|x_{\text{lead}}| > 0.8$, is expected to be enriched in collisions occurring via double-pomeron (-reggeon)

exchange processes. As follows from a comparison of full and open circles in Figs. 1a and 1b, $\langle n \rangle$ for this sub-sample practically coincides with that for the sample with $|x_{\rm lead}| > 0.5$, i.e., for the sample where semi-inclusive single diffraction dissociation dominates (note, that $M_{\rm X}^2 c^2 \approx s(1-x_{\rm M})(1-|x_{\rm p}|)$, so that the higher $|x_{\rm lead}|$ cut-off leads to a lower $M_{\rm X}$ restriction).

The present data confirm the earlier observation [14,15] that the $M_{\rm X}$-dependence of $\langle n \rangle$ is insensitive to the type of hadrons colliding (cf. Figs. 1a and 1b). Our combined $(\pi^+/{\rm K}^+){\rm p}$ data from which the two-prong events ($n = 0$) are excluded (a restriction applied for other data presented in Fig. 1c), are in good agreement with the $\overline{\rm p}{\rm p}$ data [15] and do not contradict the data obtained in $\gamma\gamma$-collisions [20]. The curve in Fig. 1c represents the ${\rm e}^+{\rm e}^-$ data fitted in the range of $M_{\rm X} \equiv \sqrt{s_{ee}}/c^2$=1.4-9.4 GeV/$c^2$ by the form $\langle n \rangle = A + B \ln M_{\rm X}^2 + C \ln^2 M_{\rm X}^2$ with $A = 2.81 \pm 0.06$, $B = 0.22 \pm 0.05$ and $C = 0.12 \pm 0.01$ ($M_{\rm X}$ in GeV/$c^2$). There is a difference between ${\rm e}^+{\rm e}^-$ and hadronic data, more strongly pronounced at low $M_{\rm X}(< 4$ GeV/$c^2)$ than at larger values. It was observed in pp-collisions (with both leading protons at $0.44 < |x_p| < 0.82$) [21] that, in the mass range $M_{\rm X} = 14 - 31$ GeV/$c^2$, the average multiplicity $\langle n \rangle$ even exceeds that observed in ${\rm e}^+{\rm e}^-$-collisions [17, 22]. This behavior of $\langle n \rangle$ in hadron-hadron collisions is generally attributed to the increasing relative contribution of the hard-like processes of scattering (absent in ${\rm e}^+{\rm e}^-$) and fragmentation (present in ${\rm e}^+{\rm e}^-$) [6].

The non-diffractive sub-sample of reaction (1) is given in Fig. 1d. The enhancement at small mass ($M_{\rm X} < 3$ GeV/$c^2$) is caused by the diffractive cut removing events with $n \leq 6$ and low $M_{\rm X}$. The curves will be discussed in Sub-Sect. 3.3.

### 3.2 Two versions of the FRITIOF model

In this and the next sections, the data on the *non-diffractive* sub-samples of reactions (1), (3) and (4) are compared with predictions of two versions of the FRITIOF model: FRITIOF2.0 [5] and FRITIOF7.0 [6]. Both models include the hard-like sub-processes of

i) parton-parton (mainly gluon-gluon) scattering (Rutherford parton scattering, RPS),

ii) associated gluon bremsstrahlung in the collision phase, and

iii) semihard gluon radiation in the fragmentation phase of the two excited (color singlet) strings which behave as a color dipole antenna.

In the *collision phase*, the colliding hadrons emerge as two excited (color singlet) strings. A primordial transverse momentum $Q_{2{\rm T}}$ is given to the string ends, which is assumed to have a Gaussian distribution with an average $\langle Q_{2{\rm T}}^2 \rangle$. In both models, we use $\langle Q_{2{\rm T}}^2 \rangle$=0.42 (GeV/c)$^2$ for the primordial transverse momentum. This value is similar to the one adopted in deep-inelastic $\mu$p and $\nu(\overline{\nu})$p interactions [3,23]. In version 7.0, soft transverse momentum transfer $Q_{\rm T}$ also takes place between colliding hadrons according to a Gaussian with $\langle Q_{\rm T}^2 \rangle$ of the size of a squared hadron mass [6]. The default value $\langle Q_{\rm T}^2 \rangle$=0.01 (GeV/$c$)$^2$ in version 7.0 seems to be too small. Even in single-diffractive scattering the squared transverse momentum acquired by the excited hadron state is $\langle Q_{\rm T}^2 \rangle$=0.1-0.15 (Gev/$c$)$^2$, while in non-diffractive processes [25] it is quoted to be 0.25-0.4 (GeV/c)$^2$. As will be shown in Sections 3.3 and 4 below, the model predictions for the transverse momentum of the leading $\pi^+$ meson badly underestimate the experimental data at the default value of $\langle Q_{\rm T}^2 \rangle$. Therefore, an attempt is undertaken to tune the parameter $\langle Q_{\rm T}^2 \rangle$ from comparison with the experimental data.

In addition, a hard parton-parton elastic scattering (Rutherford parton scattering, RPS) can take place in both versions with a comparatively large transverse momentum. The RPS involves mainly gluons. In FRITIOF7.0 an updated version of the gluon-gluon RPS with associated gluon bremsstrahlung is considered, leading to an increase of the multiplicity of particles produced in the central rapidity region and allowing [6] for the reproduction of the high-multiplicity tail of the charged-particle distribution measured in the NA22 experiment [9]. With a much smaller rate, the RPS also involves the valence quarks and can, therefore, give rise to a relatively large transverse momentum of the leading hadrons.

In the *fragmentation phase* both versions are based on a physical picture, according to which the extended string behaves as a color dipole (antenna) radiating semihard gluons [24, 6]. In the string c.m.s., the transverse momentum of radiated gluons is restricted by energy-momentum conservation, $k_\perp < (M/2)e^{-|y^*|}$ (where $M$ is the dipole mass and $y^*$ is the gluon rapidity in the string c.m.s.), and by the requirement that the gluon wavelength should exceed the transverse size $L$ of the string, $k_\perp < \sqrt{\frac{\pi M}{L}} e^{-|y^*|/2}$, where $L$ is estimated to be about $L \approx$0.6-0.9fm [6]. At our energy ($\sqrt{s}$=21.7 GeV) the mass $M$ is, according to [25], on average less than $0.1*\sqrt{s}$. Evidently, these restrictions also limit the transverse momentum of hadrons produced in string fragmentation, including hadrons with valence quark content, which can acquire a recoil $p_T$ as a result of the gluon radiation.

It should be stressed that the character of the string radiation can be influenced by the gluon RPS. This mechanism is considered in the FRITIOF7.0 version but not in FRITIOF2.0. The gluon RPS strongly disturbs the color field of the string, which now acts as two dipoles with smaller mass, radiating gluons with smaller $k_\perp$ in comparison to the case of one undisturbed string. As a consequence, FRITIOF7.0 predicts a larger fraction of events with relatively large multiplicity and relatively small transverse momentum of the produced hadrons than that found with FRITIOF2.0. As will become clear in Sects. 3.3 and 4, the prediction of the two model versions is very different for reactions (1), (3), and (4), particularly for the dependence of the average transverse momentum of the leading hadrons on their longitudinal momentum and on the multiplicity of accompanying pions.

In both versions, the width of the Gaussian $p_x$ and $p_y$ transverse momentum distributions for direct (primary) hadrons is $\sigma_x = \sigma_y = 0.37$ GeV/c as in the OPAL setting [26]. With these parameters we describe in particular the $p_T^2$ distribution of our data up to the experimentally measured values of 4.5 (GeV/c)$^2$ in the inclusive reaction $\pi^+ p \to \pi^\pm X$.

To be consistent with the experimental cuts, all particles except protons with $p_{lab} < 1.2$ GeV/c are assumed to be pions and Monte Carlo events satisfying the "diffractive" criteria [13] are excluded.

### 3.3 The comparison with model predictions

In a comparison of the experimental data with the predictions of the two versions of the FRITIOF model, the model parameters were fixed as described above, except for $\langle Q_T^2 \rangle$ (the squared transverse momentum transfer between colliding hadrons in the FRITIOF7.0 version) which was varied in the wide range of 0.01-0.3 (GeV/$c$)$^2$. The FRITIOF7.0 predictions concerning the transverse momentum of the leading hadrons (in particular, the dependence of $\langle p_T \rangle_{\rm lead}$ on $x_{\rm lead}$ and on the associated multiplicity $n$) are found to be rather sensitive to $\langle Q_T^2 \rangle$. The data on $\langle p_T \rangle_{\pi^+}$ favor larger values of $\langle Q_T^2 \rangle \geq$ 0.2-0.3 (GeV/$c$)$^2$, while the data on $\langle p_T \rangle_p$ favor smaller values of $\langle Q_T^2 \rangle \leq$ 0.1-0.2 (GeV/$c$)$^2$. In the figures below, the FRITIOF7.0 predictions are given at the default value of 0.01 (GeV/$c$)$^2$ (full lines). Distributions particularly sensitive to the value of $\langle Q_T^2 \rangle$ are also given at the "intermediate" value of $\langle Q_T^2 \rangle$ = 0.2 (GeV/$c$)$^2$ (dot-dashed). All those distributions only given for the default version either stay the same or improve slightly when increasing $\langle Q_T^2 \rangle$ to 0.2 (GeV/$c$)$^2$.

Both versions of the model (FRITIOF2.0 to a larger extent) underestimate the average charge multiplicity $\langle n \rangle$ given as a function of the effective mass $M_X$ in Fig. 1d.

Plots of the charged-particle-multiplicity and effective-mass distributions of the central system $X_n$, as well as the inclusive distributions of centrally produced charged pions are shown in Fig. 2 for the non-diffractive part of reaction (1). The multiplicity distribution (Fig. 2a) is reproduced by FRITIOF7.0, while the prediction of FRITIOF2.0 is significantly narrower and shifted toward smaller multiplicities. Both model predictions reproduce qualitatively the general trend of the $M_X$-distribution given in Fig. 2b. They are, however, shifted toward slightly higher $M_X$ values than are the data. Both versions predict a central-pion rapidity distribution wider than the one measured (Fig. 2c). The models essentially reproduce the central-pion $p_T^2$-distribution, which can be approximated by a sum of two exponentials

with slopes $b_1 = 12.2 \pm 0.7$ and $b_2 = 3.7 \pm 0.2$ (GeV/$c$)$^{-2}$ (Fig. 2d). The $p_T^2$ -distributions of centrally produced hadrons were measured at higher $M_X$ ($11 - 34$ GeV/$c^2$) in pp-collisions at $\sqrt{s} = 62$ GeV. In the "soft" region, the slope parameter $b_1$ is approximately the same, whereas in the "hard" region the spectra are flatter ($b_2 \sim 2$ (GeV/$c$)$^{-2}$) than those in our experiment (at $M_X < 10$ GeV/$c^2$).

The characteristics of the leading hadrons produced in the non-diffractive sub-sample of reaction (1) are presented in Fig. 3. Both versions of the model essentially reproduce the $x$-distribution of the leading pion (Fig. 3a). However, the predictions for the leading proton are shifted toward smaller values of $|x_p|$ (Fig. 3b). The $p_T^2$-distribution for the leading pion, shown in Fig. 3c, can be approximated by a sum of two exponentials with slopes $b_1^\pi = 6.2 \pm 0.8$ and $b_2^\pi = 1.7 \pm 0.4$ (GeV/$c$)$^{-2}$. Both versions of the model fail in describing the high $p_T^2$ -tail of this distribution. The models qualitatively reproduce the single-exponential shape of the $p_T^2$ -distribution of the leading proton (Fig. 3d). They predict, however, a somewhat smaller slope parameter than the $b_p = 5.9 \pm 0.2$ (GeV/$c$)$^2$ extracted from the data.

The average transverse momentum $\langle p_T \rangle$ of the leading hadrons does not vary significantly with the charged particle multiplicity $n$ of the central system $X_n$ (Figs. 3e and 3f). This trend is roughly reproduced by FRITIOF2.0. On the other hand, FRITIOF7.0 reproduces the behavior of the leading protons in Fig. 3f, but largely underestmates $\langle p_T \rangle$ for the leading $\pi^+$ in Fig. 3e. Changing $\langle Q_T^2 \rangle$ from its default value of 0.01 (GeV/$c$)$^2$ to 0.2 (GeV/$c$)$^2$ (dot-dashed lines) improves the situation for the $\pi^+$, but now overestimates the proton $\langle p_T \rangle$.

In Fig. 4, the $x$-dependence of $\langle p_T \rangle$ for leading hadrons and central pions produced in the non-diffractive sub-sample of reaction (1) is compared with that found in the diffractive-enriched sample ($|x_{lead}| > 0.8$). Leading hadrons acquire a larger transverse momentum in the non-diffractive sample. However, centrally produced pions ($|x| < 0.15$) have approximately the same $\langle p_T \rangle$ in both reactions.

Both versions of the model reproduce the general trends of the data for central pions; in particular, the model reproduces the observed asymmetry in $\langle p_T \rangle$ with respect to positive- and negative-$x$ regions.

FRITIOF2.0 shows reasonable agreement with the data for the leading pion at $x < 0.8$, but underestimates the data at $x > 0.8$. The predictions of FRITIOF7.0 (default) are too low over the whole range of the leading pion ($x > 0.5$) and tend to underestimate the leading proton data at $x < -0.85$. Increasing $\langle Q_T^2 \rangle$ to 0.2 (GeV/$c$)$^2$ (dot-dashed lines) improves $\langle p_T \rangle$ for the leading pions, but, again, largely overshoots for the leading protons at $x < -0.7$.

In conclusion, the multiplicity and semi-inclusive characteristics of reaction (1) are not reproduced by the model with a unique set of input parameters.

# 4 Reactions with a single leading hadron

The multiplicity distribution of $X_n$ and the inclusive characteristics of the non-leading charged pions accompanying the production of a single leading hadron in the non-diffractive sample of reactions (3) and (4) are plotted in Fig. 5. As for the case of reaction (1), the FRITIOF2.0 version badly underestimates the charge multiplicity (Figs. 5a,b) and predicts a wider rapidity distribution (Figs. 5c,d), while FRITIOF7.0 significantly improves the consistency with the data. The $p_T^2$-distribution of associated pions, like that of central pions produced in reaction (1), has a double-exponential form (Figs. 5e,f), with similar slopes: $b_1 = 14.2 \pm 0.3$ and $b_2 = 3.7 \pm 0.1$ (GeV/$c$)$^{-2}$ in reaction (3) and $b_1 = 13.7 \pm 0.3$ and $b_2 = 3.6 \pm 0.1$ (GeV/$c$)$^{-2}$ in reaction (4). Both model versions essentially reproduce the non-single exponential form of the $p_T^2$-distribution.

Figs. 6a and 6b show the average charge multiplicity $\langle n \rangle$ versus the effective mass $M_X$ calculated from (6), for reactions (3) and (4), respectively. The enhancement in the range $M_X < \sqrt{s}(1 - 0.88)^{1/2}/c^2 \approx 7.5$ GeV/$c^2$ reflects the selection criteria for non-diffractive events, from which the low-multiplicity single-diffractive events (containing a leading hadron with $|x_{lead}| > 0.88$) are excluded.

For $M_X = 8 - 16$ GeV/$c^2$, the multiplicity in reaction (3) with a leading proton noticeably exceeds that in reaction (4) with a leading $\pi^+$ meson. Again, the FRITIOF2.0 version predicts multiplicities that are too low, while the FRITIOF7.0 version significantly improves the description.

The inclusive spectra of the leading hadron are shown in Figs. 6c to 6f. As was the case for reaction (1), the model predictions for the $x_p$-distribution in reaction (3) is shifted toward smaller values of $|x_p|$ (Fig. 6c). Both model versions also fail to satisfactorily describe the $x_{\pi^+}$-distribution in reaction (4) (Fig. 6d). The $p_T^2$-distribution of the leading proton in reaction (3) (Fig. 6e) and of the leading $\pi^+$ in reaction (4) (Fig. 6f) are similar to those for the leading proton and $\pi^+$ in reaction (1), respectively, and can be approximated by a single-exponential curve with a slope $b_p = 6.0 \pm 0.1$ (GeV/$c$)$^{-2}$ and by a double-exponential with slopes $b_1^\pi = 5.4 \pm 0.6$ and $b_2^\pi = 1.9 \pm 0.5$ (GeV/$c$)$^{-2}$, respectively. The FRITIOF2.0 version essentially reproduces the $p_T^2$-distributions, except perhaps for the leading $\pi^+$ at $p_T^2 > 1$ (GeV/$c$)$^2$. FRITIOF7.0 fails in reproducing the $p_T^2$-distributions, especially for the leading $\pi^+$, being too strongly peaked at small $p_T^2$. With $\langle Q_T^2 \rangle = 0.2$ (GeV/$c$)$^2$, FRITIOF7.0 qualitatively reproduces the data for the leading $\pi^+$, but the prediction for the leading proton is now flatter than that found by experiment. We checked that the 7.0 version at $\langle Q_T^2 \rangle$ =0.1 (GeV/$c$)$^2$ can describe the $p_T^2$-distribution for the leading proton, but it still fails in describing that for the leading pion.

The average transverse momentum $\langle p_T \rangle_p$ of the leading proton (Fig. 7a) is independent of the charge multiplicity $n$, except for $n = 1$. Both models predict the independence of $n$, but FRITIOF2.0 overestimates and FRITIOF7.0 underestimates the value. Again, FRITIOF7.0 with $\langle Q_T^2 \rangle = 0.2$ (GeV/$c$)$^2$ overestimates $\langle p_T \rangle$ for the leading proton. Both the experimental data and FRITIOF2.0 show a tendency of $\langle p_T \rangle_{\pi^+}$ to rise with increasing $n$ (Fig. 7b). The violent disagreement of FRITIOF7.0 (solid line) for the leading $\pi^+$ in Fig. 7b is remedied for the most part by increasing $\langle Q_T^2 \rangle$ to 0.2 (GeV/$c$)$^2$ (dot-dashed line).

In Figs. 7c and 7d, plots of the $x$-dependence of $\langle p_T \rangle$ for the leading hadrons and the associated pions are shown. The associated pions carry larger $\langle p_T \rangle$ in the hemisphere opposite to the leading hadron than in the same hemisphere. This forward-backward asymmetry in $\langle p_T \rangle$ is essentially reproduced by FRITIOF2.0, but not by FRITIOF7.0. In the most central region of $|x| < 0.1$, the average transverse momentum is practically the same in reactions (3), (4) as in reaction (1) (cf. Fig. 4), and only slightly lower in this case than in the non-diffractive inclusive reaction $\pi^+ p \rightarrow \pi^\pm + X$ in the same experiment [7]. This region is qualitatively reproduced by the models. FRITIOF2.0 also roughly describes the data in the region $|x|$= 0.1-0.4 for reaction (4) (Fig. 7d), but underestimates the data for reaction (3) (Fig. 7c). FRITIOF7.0 fails in describing the data, particularly in the region of $x > 0.2$ for both reactions (3) and (4).

The $x$-dependence of $\langle p_T \rangle_p$ for the leading proton in reaction (3) (Fig. 7c) and of $\langle p_T \rangle_{\pi^+}$ for the leading pion in reaction (4) (Fig. 7d) do not differ significantly from that for reaction (1). Both model versions fail in describing the $x$- dependence of $\langle p_T \rangle_p$: FRITIOF7.0 significantly underestimates the data for $x < -0.7$, but overestimates them almost over the whole range of $x_p$ for $\langle Q_T^2 \rangle = 0.2$ (GeV/$c$)$^2$, while FRITIOF2.0 predicts a strongly falling dependence at $x_p < -0.7$ and badly underestimates the data at $x_p < -0.9$ (Fig. 7c). The $\langle p_T \rangle_{\pi^+}$ data are violently underestimated by the default FRITIOF7.0 version but reproduced with $\langle Q_T^2 \rangle = 0.2$ (GeV/$c$)$^2$, while FRITIOF2.0 badly underestimates the data at $x_{\pi^+} > 0.8$ (Fig.7d).

Note that similar to reaction (1), for reaction (3) the description of the data concerning the transverse momentum of the leading proton (Figs. 6e, 7a and 7c) could also be significantly improved in FRITIOF7.0 at a value of the parameter $\langle Q_T^2 \rangle$ of $\leq 0.1$ (GeV/$c$)$^2$. However, in this case, the model fails badly in describing the data concerning the transverse momentum of the leading pion in reaction (4); in particular, the model drastically underestimates the data on $\langle p_T \rangle_{\pi^+}$ plotted in Figs. 7b and 7d (not shown).

# 5 Summary

Inelastic final states with a single or two leading hadrons have been studied in $\pi^+$p and $K^+$p interactions at 250 GeV/$c$.

The dependence of the mean charged particle multiplicity $\langle n \rangle$ of the associated pion system on its effective mass $M_X$ in reactions with two leading hadrons in the final state is consistent with that measured earlier at lower incident momenta. This dependence is insensitive to the type of colliding hadrons and to the cut applied on the Feynman-$x$ variable of the leading hadrons. It is also consistent with that observed for $\gamma\gamma$-collisions. The average multiplicity $\langle n \rangle$ is noticeably lower in hadronic collisions than in the hard process of $e^+e^-$-annihilation. However, the difference between the two sets of data tends to be reduced with increasing $M_X$.

The $p_T^2$-distributions of associated pions in $\pi^+$-induced non-diffractive reactions with a single or two leading hadrons have a characteristic double-exponential form with slope parameters $b_1 \approx 12 - 14$ (GeV/$c$)$^{-2}$ and $b_2 \approx 3.6 - 3.8$ (GeV/$c$)$^{-2}$. A similar double-exponential form, but with a flatter slope ($b_2 \sim 2$ (GeV/$c$)$^{-2}$) in the large $p_T^2$-range, was observed earlier in pp-collisions at $\sqrt{s} = 62$ GeV. Both versions of the FRITIOF model essentialy reproduce this double-exponential shape.

The multiplicity characteristics of associated pions are not reproduced by the FRITIOF2.0 version, which predicts too low $\langle n \rangle$ in the whole available $M_X$ range for all non- diffractive reactions considered. FRITIOF7.0 significantly improves the description of the multiplicity characteristics. This is achieved by means of the updated hard-like mechanisms of the RPS and its influence on the gluon radiation by excited strings (see Sect. 3 above), providing a larger multiplicity of produced pions.

On the other hand, these mechanisms themselves lead to a smaller transverse momentum of the leading hadrons (as compared with FRITIOF2.0) and drastically worsen the predictive power of the FRITIOF7.0 version (at the default value of $\langle Q_T^2 \rangle$=0.01 (GeV/$c$)$^2$) for the transverse momentum distribution of the leading $\pi^+$ meson. Further improvement of the predictive power of the model could be achieved by tuning the parameter $\langle Q_T^2 \rangle$ on experimental data concerning the transverse momentum of final hadrons (note that the other characteristics of the reactions considered are not sensitive to the choice of $\langle Q_T^2 \rangle$).

An attempt of this tuning, undertaken in the present work, shows that:

i) the data concerning $\langle p_T \rangle_p$ favor a "moderate" value of $\langle Q_T^2 \rangle \leq 0.1$ (GeV/$c$)$^2$, at which, however, the predicted magnitude of $\langle p_T \rangle_{\pi^+}$ still turns out to be badly underestimated;

ii) the data concerning $\langle p_T \rangle_{\pi^+}$ favor a larger value of $\langle Q_T^2 \rangle \geq 0.2$ (GeV/$c$)$^2$, at which the predicted magnitude of $\langle p_T \rangle_p$ already turns out to be significantly overestimated;

iii) the $x$- dependence of $\langle p_T \rangle$ for associated pions in reactions with a single leading hadron cannot be satisfactorily described at any value of $\langle Q_T^2 \rangle$.

The current versions of the FRITIOF fragmentation model, therefore, do not reproduce simultaneously (with a unique set of input parameters) the semi-inclusive characteristics of non-diffractive meson-proton collisions with leading hadrons in the final state. The hard-like sub-processes of parton scattering and gluon radiation do not seem properly treated in the model.

# 6 Acknowledgments

We are grateful to the III. Physikalisches Institut B, RWTH Aachen, Germany, the DESY-Institut für Hochenergiephysik, Berlin-Zeuthen, Germany; the Department of High Energy Physics, Helsinki University, Finland; the Institute for High Energy Physics, Protvino, Russia; and the University of Warsaw and Institute of Nuclear Problems, Poland for early contributions to this experiment. This work is part of the research program of the "Stichting voor Fundamenteel Onderzoek der Materie (FOM)", which is financially supported by the "Nederlandse Organisatie voor Wetenschappelijk Onderzoek

(NWO)". We further thank NWO for support of this project within the program for subsistence to the former Soviet Union (07-13-038). The Yerevan group activity is financially supported, in the framework of the theme No. 94-496, by the Government of the Republic of Armenia.

## References

[1] M. Althoff et al.: Z. Phys. C22 (1984) 307

[2] M. Derrick et al.: Phys. Rev. D17 (1978) 1
P. Allen et al.: Nucl. Phys. B188 (1981) 1
D. Allasia et al.: Z. Phys. C27 (1985) 239

[3] M. Arneodo et al.: Phys. Lett. B149 (1984) 415

[4] I.V. Ajinenko et al., NA22 Coll.: Phys. Lett. B197 (1987) 457

[5] B. Andersson, G. Gustafson and B. Nilsson-Almqvist: Nucl. Phys. B281 (1987) 289

[6] B. Andersson, G. Gustafson and Hong Pi: Z. Phys. C57 (1993) 485

[7] N.M. Agababyan et al., NA22 Coll.: Phys. Lett.B320 (1994) 411

[8] M. Aguilar-Benitez et al.: Nucl. Instrum. Methods 205 (1983) 79

[9] M. Adamus et al., NA22 Coll.: Z. Phys. C32 (1986) 475

[10] M. Adamus et al., NA22 Coll.: Z. Phys. C39 (1988) 311

[11] M. Adamus et al., NA22 Coll.: Phys. Lett. B186 (1987) 223

[12] N. Agababyan et al., NA22 Coll.: Z. Phys. C60 (1993) 229

[13] M. Adamus et al., NA22 Coll.: Z. Phys. C39 (1988) 301

[14] D. Brick et al.: Phys. Lett. 103B (1981) 241

[15] S.V. Chekulaev et al.: Yad. Fis. 49 (1989) 452

[16] C. Bacci et al.: Phys. Lett. 86B (1979) 234

[17] Ch. Berger et al.: Phys. Lett. 95B (1980) 313

[18] B. Niczyporuk et al.: Z. Phys. C9 (1981) 1

[19] J.L. Siegrist et al.: Phys. Rev. D26 (1982) 969

[20] S.E. Baru et al.: Z. Phys. C53 (1992) 219

[21] A. Breakstone et al.: Z. Phys. C11 (1981) 203

[22] R. R. Brandelik et al.: Phys. Lett. 89B (1980) 412; 83B (1979) 261

[23] M. Arneodo et al.: Z. Phys. C36 (1987) 527

[24] G. Gustafson: Nucl. Phys. B (Proc. Suppl.) 16 (1990) 441

[25] I.V. Ajinenko et al., NA22 Coll.: Z. Phys. C49 (1991) 367

[26] M.Z. Akrawy et al.: Z. Phys. C47 (1990) 505

# Figure captions

Fig. 1. The dependence of the average charged particle multiplicity $\langle n \rangle$ on the effective mass $M_X$ of the centrally produced system $X_n$ for a) $\pi^+ p \to \pi^+_{lead}\, p_{lead}\, X_n$, b) $K^+ p \to K^+_{lead}\, p_{lead}\, X_n$, c) our data with $n \geq 2$ compared to those obtained in $p\bar{p}$ [15], $e^+e^-$ [16-19] and $\gamma\gamma$ [20] collisions, d) the non-diffractive $\pi^+ p$ sample compared to the predictions from two versions of the FRITIOF model.

Fig. 2. The characteristics of the central system $X_n$ produced in non-diffractive $\pi^+ p \to \pi^+_{lead}\, p_{lead}\, X_n$ reactions: a) charged particle multiplicity of $X_n$, b) effective mass of $X_n$, c) charged-pion rapidity within $X_n$, d) squared transverse momentum of charged pions produced in $X_n$.

Fig. 3. The characteristics of the leading pion (a,c,e) and proton (b,d,f) produced in non-diffractive $\pi^+ p \to \pi^+_{lead}\, p_{lead}\, X_n$ reactions: a) and b) Feynman-$x$ dependence, c) and d) squared-transverse-momentum dependence e) and f) average transverse momentum as a function of the charged particle multiplicity of $X_n$.

Fig. 4. The $x$- dependence of $\langle p_T \rangle$ (the "sea-gull") for leading hadrons and associated pions in the non-diffractive sample of reaction (1). Circles: $|x_{lead}| > 0.5$; crosses: $|x_{lead}| > 0.8$.

Fig. 5. The characteristics of the system $X_n$ accompanying the production of a single leading hadron: a) and b) charged particle multiplicity of $X_n$, c) and d) charged-pion rapidity within $X_n$, e) and f) squared transverse momentum of charged pions produced in $X_n$.

Fig. 6. a) and b) The average charged particle multiplicity of the system $X_n$ accompanying the production of a single leading hadron, as a function of its effective mass $M_X$, c) and d) Feynman-$x$ of the single leading hadron, e) and f) squared transverse momentum of the single leading hadron.

Fig. 7. a) and b) The average transverse momentum of the leading single hadron as a function of the charged particle multiplicity $n$ of the accompanying system $X_n$, c) and d) the average transverse momentum as a function of Feynman-$x$ for the single leading hadron (solid circles) and the associated charged pions (crosses).

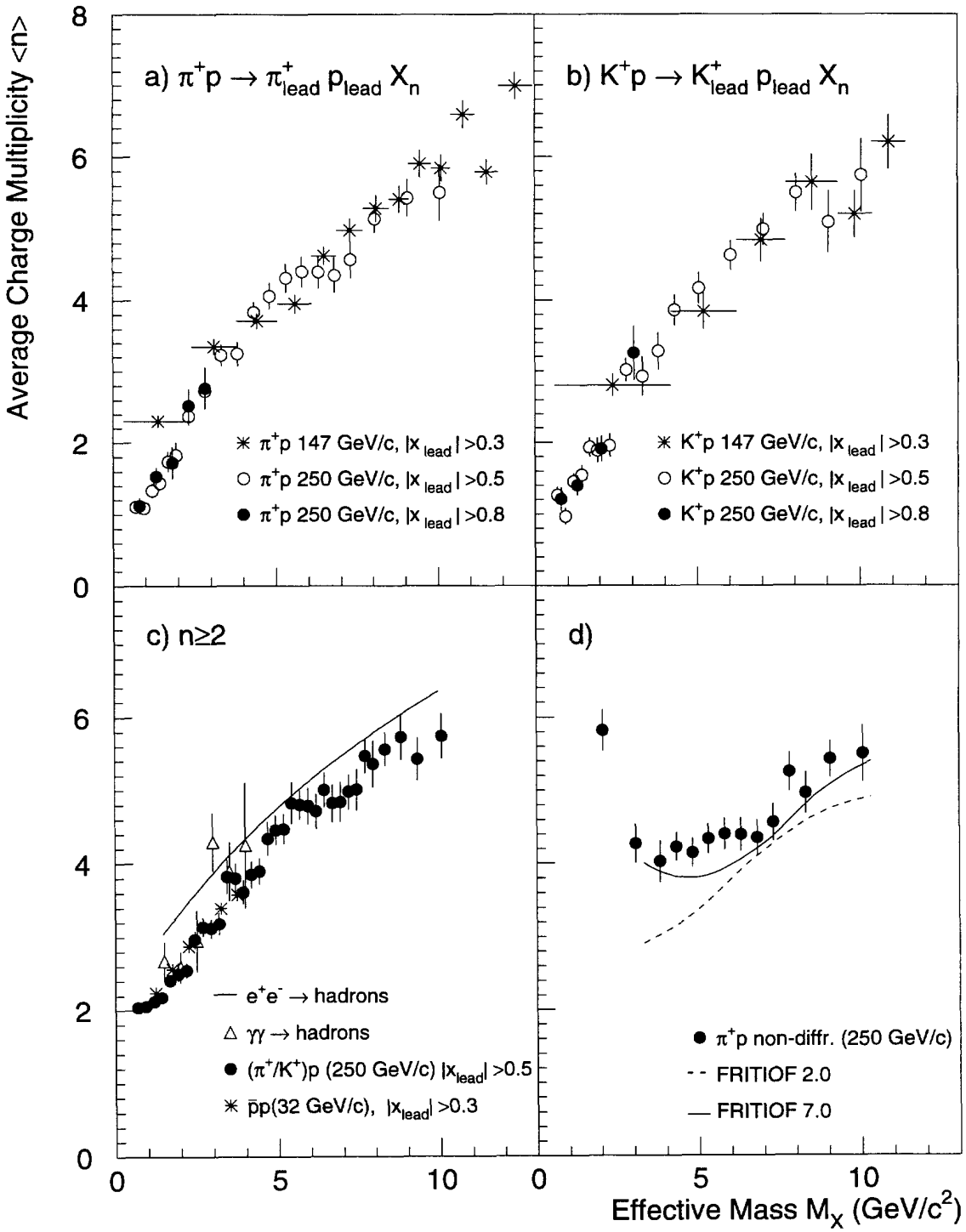
Average Charge Multiplicity <n>
a) $\pi^+p \to \pi^+_{lead}\, p_{lead}\, X_n$
b) $K^+p \to K^+_{lead}\, p_{lead}\, X_n$
$\pi^+p$ 147 GeV/c, $|x_{lead}|>0.3$
$\pi^+p$ 250 GeV/c, $|x_{lead}|>0.5$
$\pi^+p$ 250 GeV/c, $|x_{lead}|>0.8$
$K^+p$ 147 GeV/c, $|x_{lead}|>0.3$
$K^+p$ 250 GeV/c, $|x_{lead}|>0.5$
$K^+p$ 250 GeV/c, $|x_{lead}|>0.8$
c) n≥2
d)
$e^+e^- \to$ hadrons
$\gamma\gamma \to$ hadrons
$(\pi^+/K^+)p$ (250 GeV/c) $|x_{lead}|>0.5$
$\bar{p}p$(32 GeV/c), $|x_{lead}|>0.3$
$\pi^+p$ non-diffr. (250 GeV/c)
FRITIOF 2.0
FRITIOF 7.0
Effective Mass $M_X$ (GeV/$c^2$)

Fig. 1

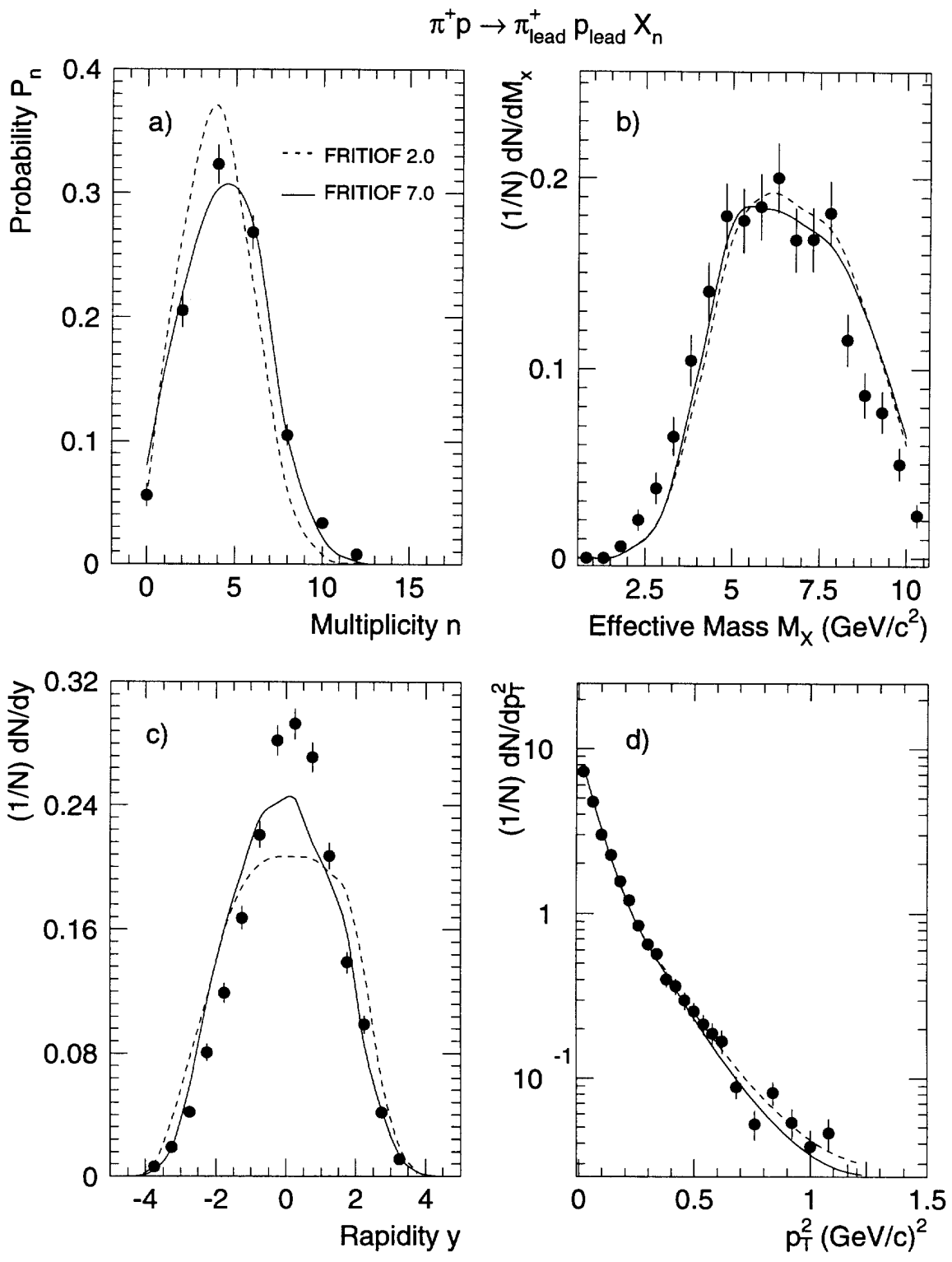
$\pi^+ p \rightarrow \pi^+_{lead}\, p_{lead}\, X_n$
a)
FRITIOF 2.0
FRITIOF 7.0
Probability $P_n$
Multiplicity n
b)
(1/N) dN/dM$_x$
Effective Mass $M_X$ (GeV/c$^2$)
c)
(1/N) dN/dy
Rapidity y
d)
(1/N) dN/dp$_T^2$
$p_T^2$ (GeV/c)$^2$

Fig. 2

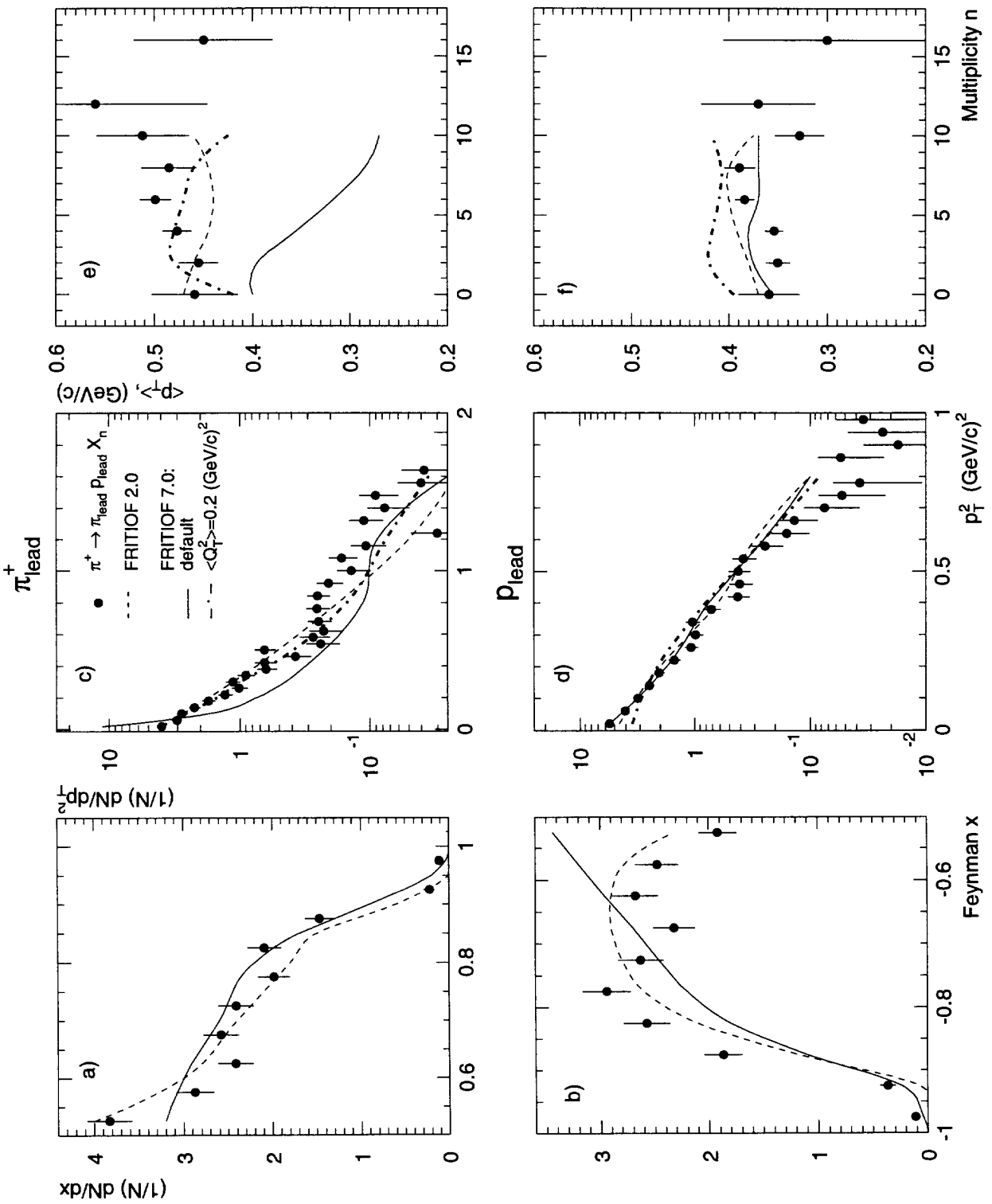
a)
b)
c)
d)
e)
f)
$\pi^+_{lead}$
$p_{lead}$
$\pi^+ \to \pi_{lead}\, p_{lead}\, X_n$
FRITIOF 2.0
FRITIOF 7.0:
default
$\langle Q^2_T \rangle = 0.2$ (GeV/c)$^2$
$\frac{1}{N} dN/dx_F$
$\frac{1}{N} dN/dp_T^2$
$\langle p_T \rangle$, (GeV/c)
$p_T^2$ (GeV/c)$^2$
Feynman x
Multiplicity n

Fig. 3

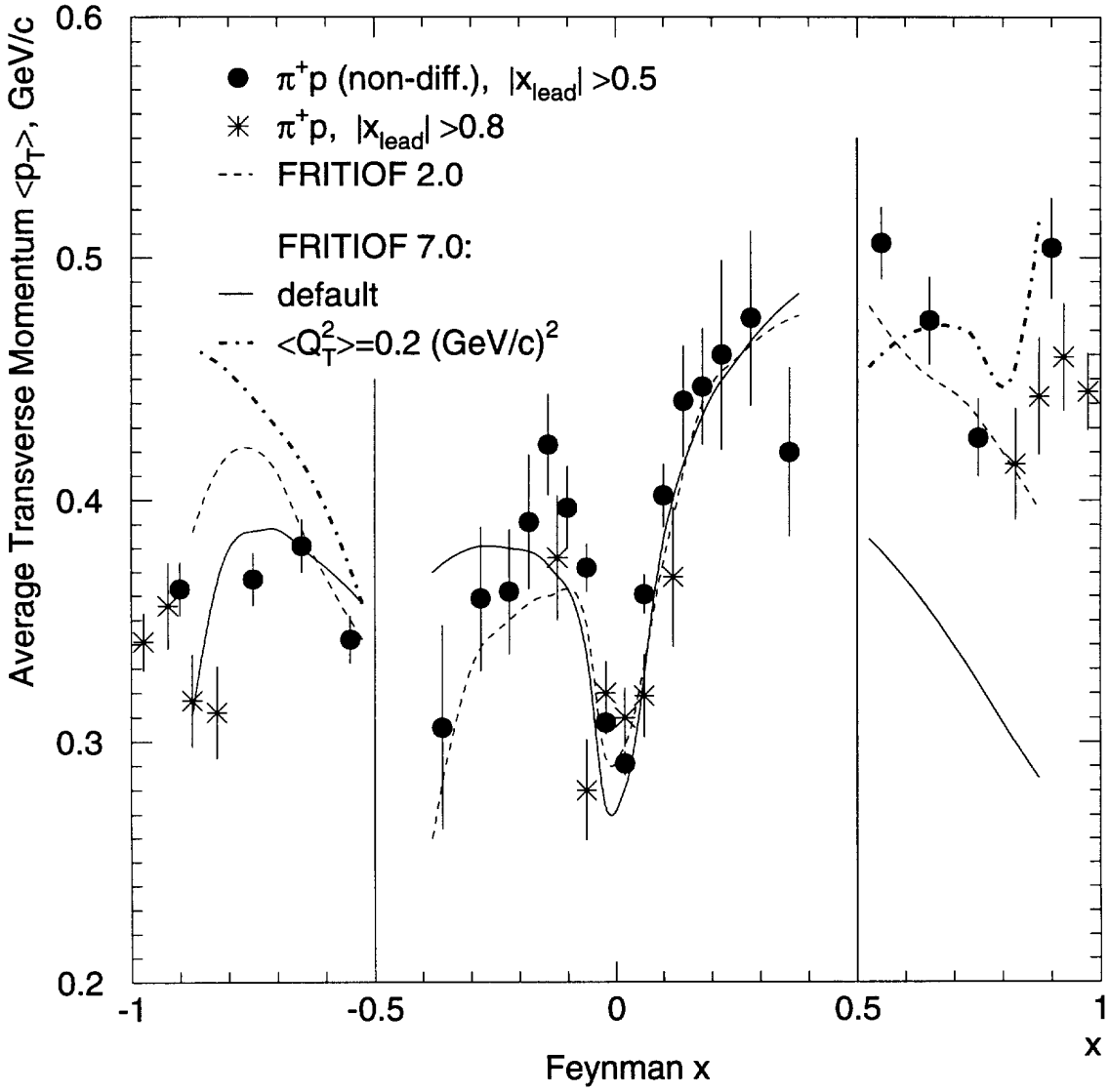
0.6
0.5
0.4
0.3
0.2
Average Transverse Momentum <p_T>, GeV/c
π+p (non-diff.), |x_lead| >0.5
π+p, |x_lead| >0.8
FRITIOF 2.0
FRITIOF 7.0:
default
<Q_T^2>=0.2 (GeV/c)^2
-1
-0.5
0
0.5
1
x
Feynman x

Fig. 4

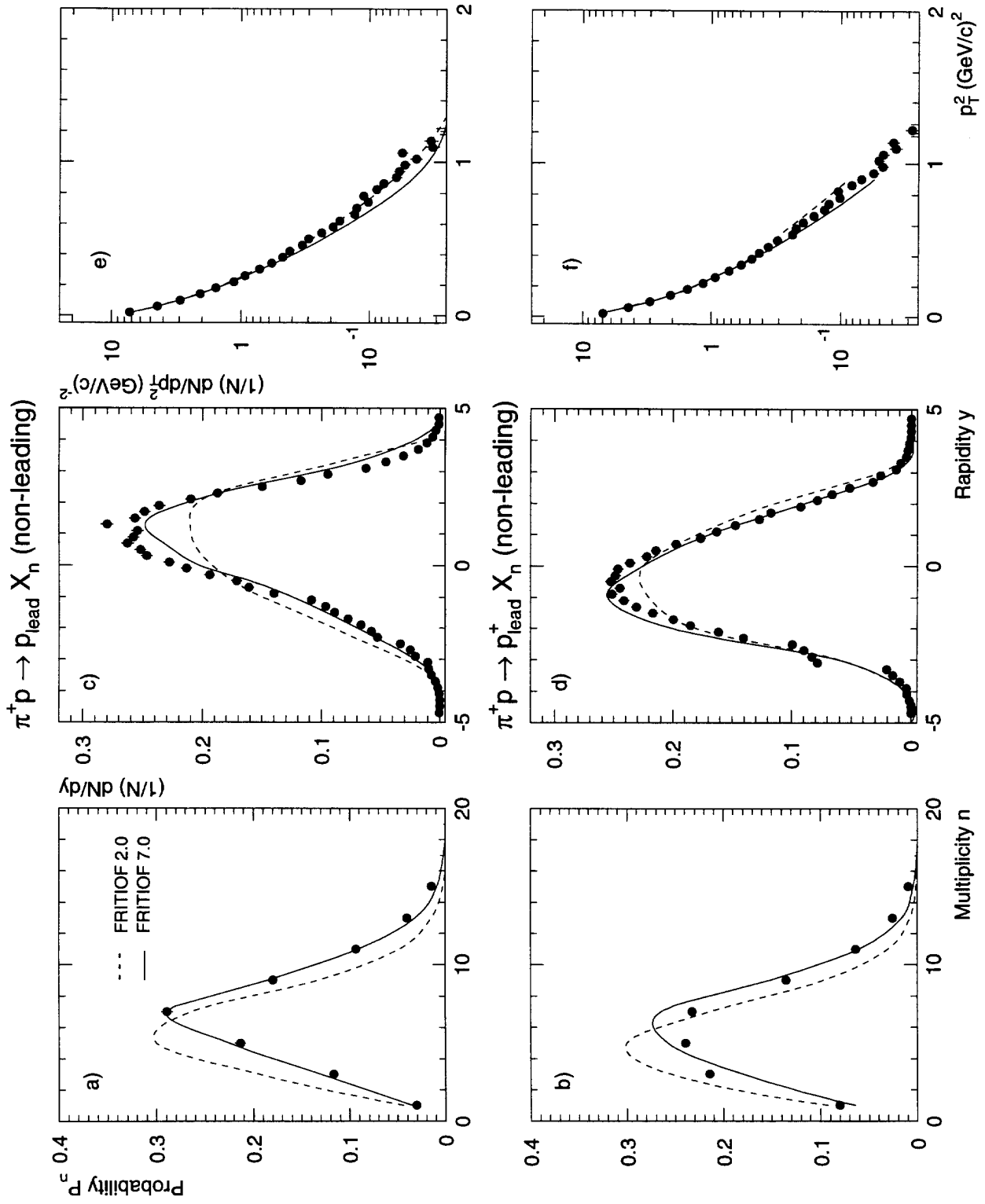
a)
b)
c)
d)
e)
f)
FRITIOF 2.0
FRITIOF 7.0
Probability P_n
(1/N) dN/dy
(1/N) dN/dp_T^2 (GeV/c)^-2
π+p → p_lead X_n (non-leading)
π+p → p+_lead X_n (non-leading)
Multiplicity n
Rapidity y
p_T^2 (GeV/c)^2

Fig. 5

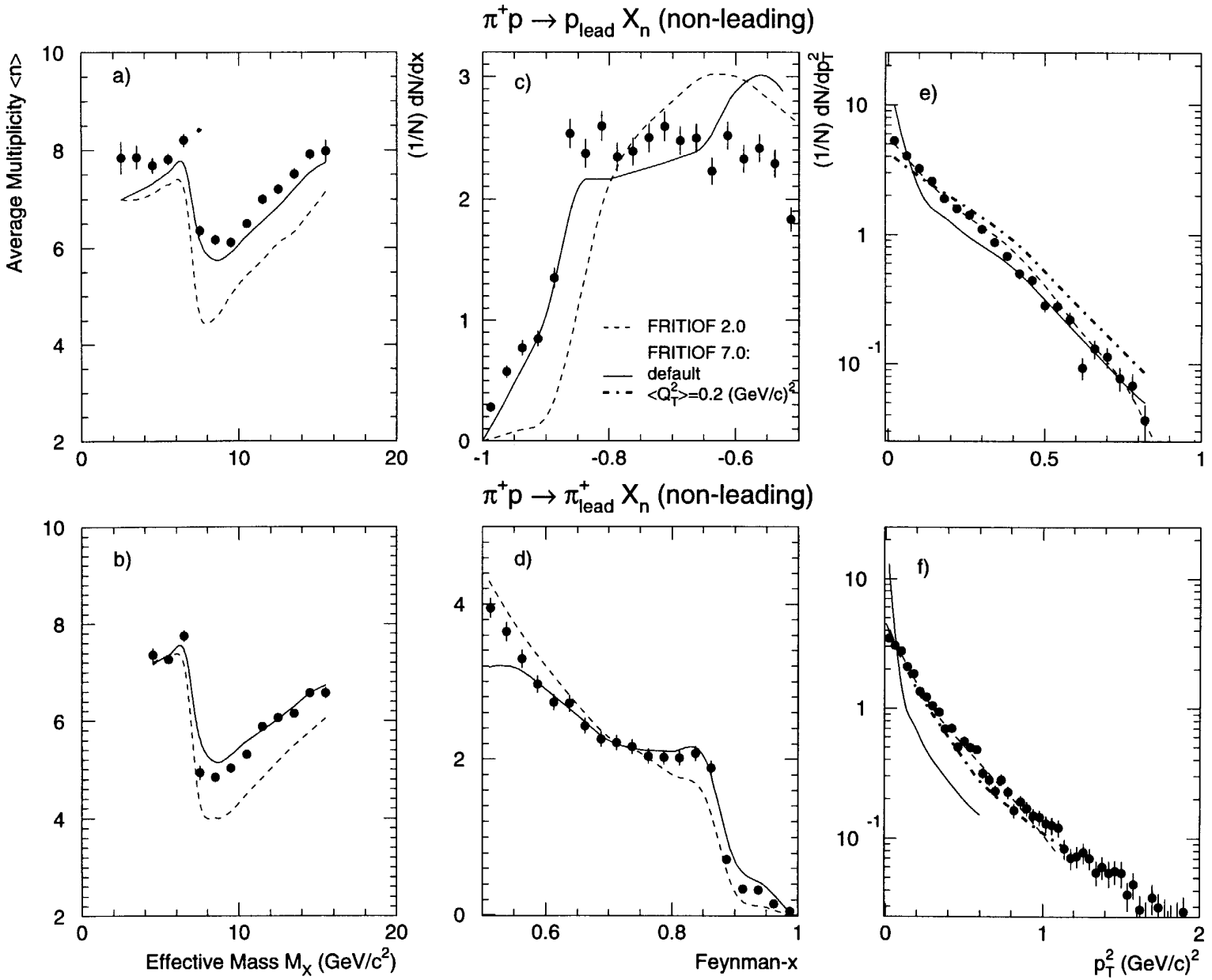
$\pi^+p \rightarrow p_{lead} X_n$ (non-leading)
$\pi^+p \rightarrow \pi^+_{lead} X_n$ (non-leading)
a)
b)
c)
d)
e)
f)
Average Multiplicity <n>
(1/N) dN/dx
(1/N) dN/dp$_T^2$
Effective Mass $M_X$ (GeV/c$^2$)
Feynman-x
$p_T^2$ (GeV/c)$^2$
FRITIOF 2.0
FRITIOF 7.0:
default
<$Q_T^2$>=0.2 (GeV/c)$^2$

Fig. 6

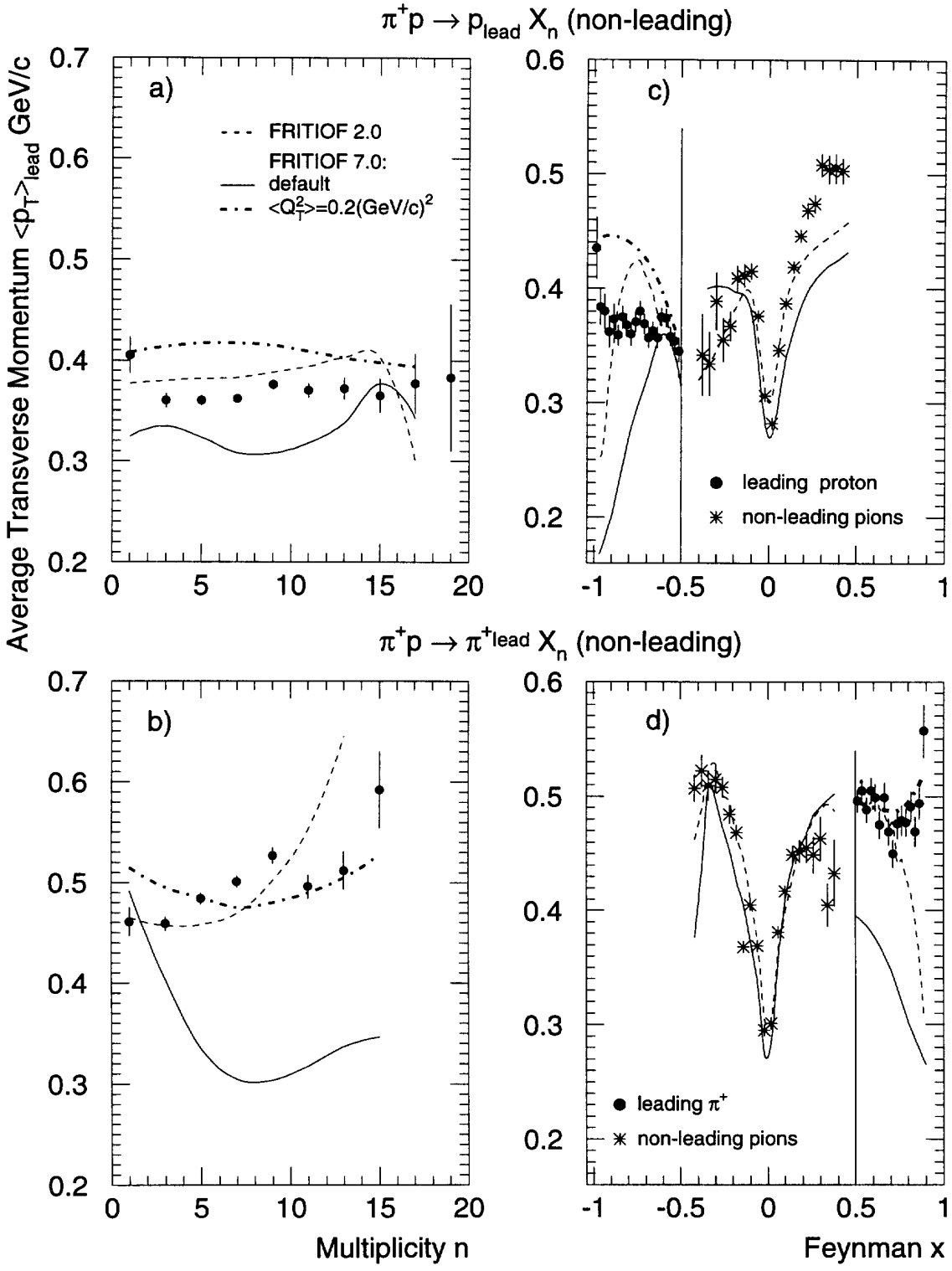
$\pi^+p \rightarrow p_{lead}\, X_n$ (non-leading)
Average Transverse Momentum $\langle p_T \rangle_{lead}$ GeV/c
a)
FRITIOF 2.0
FRITIOF 7.0:
default
$\langle Q_T^2 \rangle = 0.2(GeV/c)^2$
c)
leading proton
non-leading pions
$\pi^+p \rightarrow \pi^{+lead}\, X_n$ (non-leading)
b)
d)
leading $\pi^+$
non-leading pions
Multiplicity n
Feynman x

Fig. 7